Geomech. Geophys. Geo-energ. Geo-resour. (2023) 9:114
https://doi.org/10.1007/s40948-023-00655-8

RESEARCH

Effects of ice content on compression characteristics of frozen sandstone by in-situ NMR technology

Bei Qiu · Lifeng Fan · Congming Ma · Qihao Yang · Xiuli Du

Received: 12 June 2023 / Accepted: 26 August 2023

Abstract In cold regions, the freezing of pore water in rock affects the mechanical behavior of the rock. This paper studied the ice content of frozen sandstone at different temperatures and its effects on the mechanical properties of sandstone. First, the progressive freezing treatment (from 25.0 to − 30.0 °C) and in-situ nuclear magnetic resonance test were conducted to study the evolution of the ice content of sandstone with temperature. This evolution was quantitatively described by the frozen ratio defined as the percentage of the mass of ice and the total mass of water. Then, the mechanical properties of frozen sandstone at different temperatures (25.0 °C, 0.0 °C, − 5.0 °C, − 10.0 °C, − 20.0 °C and − 30.0 °C, respectively) were tested, such as P-wave velocity, uniaxial compressive strength (UCS), peak strain and elastic modulus. Finally, the effects of the frozen ratio on these properties were discussed. The results show that the pore water in sandstone shows three stages as the temperature decreases: stable liquid (from 25.0 to 0.0 °C), sharp phase transition (from 0.0 to − 2.5 °C) and slow phase transition (from − 2.5 to − 30.0 °C). Especially, the capillary and bulk water in sandstone is almost completely frozen in the sharp phase transition stage. As the temperature decreases, the frozen ratio first remains constant, then increases rapidly and finally increases slowly. Moreover, as the frozen ratio increases, the P-wave velocity, UCS and peak strain increase while the elastic modulus decreases. Interestingly, the compressive failure mode of sandstone changes from brittle to ductile as the frozen ratio increases.

Highlights

1. In-situ NMR tests were performed on sandstone under low temperatures.
2. Evaluate of ice content of sandstone with temperature was studied.
3. Effects of ice content on mechanical properties of sandstone were discussed.

Keywords In-situ NMR technology · Low temperature · Sandstone · P-wave velocity · Compression characteristics

1 Introduction

In high-latitude and high-altitude regions, geotechnical engineering, such as slope excavation, tunnelling and mine construction, often faces the challenges caused by extremely cold environments (Wu et al. 2010; Kodama et al. 2013; Fan et al. 2017, 2018,

B. Qiu · L. Fan (✉) · C. Ma · Q. Yang · X. Du
Faculty of Architecture, Civil and Transportation Engineering, Beijing University of Technology, Beijing 100124, China
e-mail: fanlifeng@bjut.edu.cn

Published online: 12 September 2023

2020; Lu and Cai. 2019; Chen et al. 2022). Long-term exposure to subzero environments forces rock masses to remain permanently frozen and induces a series of thermal-related responses in rock masses (Matsuoka. 1990; Ozbek. 2014; Deprez et al. 2020; Maji and Murton. 2021; Chen et al. 2023). These thermal-related responses mainly include the migration and phase transition of pore water, frost heave cracking of rock skeleton and shrinkage of mineral particles, which may further affect the mechanical behavior of rock masses under loading. Therefore, it is significant to investigate the mechanical characteristics of frozen rock and reveal the influence mechanism of temperature on frozen rock to ensure the safety and stability of engineering rock masses (Zhang and Zhao. 2020; Zhao et al. 2021; Zhong et al. 2023; Xu et al. 2023a, b).

The physical and mechanical characteristics of frozen rock, such as thermal characteristics (Park et al. 2004; Shen et al. 2018; Abdulagatova et al. 2010, 2020), wave propagation characteristics (Inada and Yokota. 1984; Draebing and Krautblatter. 2012; Huang et al. 2023), static mechanical properties (Yamabe and Neaupane. 2001; Kodama et al. 2013; Bai et al. 2020a, b; Wu et al. 2023) and dynamic mechanical properties (Shan et al. 2019; Weng et al. 2019; Xu et al. 2022; Xu et al. 2023a, b), have been extensively studied in the past decades. Specifically, some studies show that freezing can enhance the thermal conductivity of sandstone. The thermal conductivity of sandstone gradually increases with decreasing temperature, regardless of whether the sandstone is dry or water-saturated. At different temperatures, especially in the range of − 10.0–5.0 °C, the thermal conductivity of water-saturated sandstone shows a rapid increase and is larger than that of dry sandstone. This phenomenon indicates that the freezing of pore water significantly affects the thermal conductivity of sandstone (Shen et al. 2018). Meanwhile, the ultrasonic velocities of frozen sandstone were investigated. These studies show that as the temperature decreases, the P-wave and S-wave velocities of sandstone first remain almost constant (from 20.0 to 0.0 °C) and then increase (from 0.0 to − 25.0 °C). Most of the increases in P-wave and S-wave velocities occur in the range of 0.0 to − 5.0 °C. The increase in ultrasonic velocity indicates that the compactness of sandstone is enhanced in low-temperature environments. In addition, these studies also find that the ultrasonic velocity is a good parameter to describe the freezing and thawing processes of pore water in sandstone and the estimation model based on the ultrasonic velocity can accurately predict the unfrozen water content of sandstone at low temperatures (Huang et al. 2023). Furthermore, many efforts have been made to study the static mechanical properties of frozen sandstone. These studies show that the static mechanical strengths of frozen sandstone, such as static compressive strength and static tensile strength, are larger than those of natural sandstone and gradually increase with the decrease in frozen temperature (Bai et al.2020a and b; Wang et al. 2021). However, for the soft sandstone with smaller tensile strength, the freezing of pore water may cause frost heave damage to the sandstone skeleton, further weakening the resistance to deformation of sandstone (Yamabe and Neaupane. 2001; Li et al. 2021). With the development of experimental techniques, the effects of pore water freezing on the dynamic mechanical characteristics of rock were studied in-depth. In particular, the in-situ impact system equipped with the low-temperature device provides an effective method for the relevant studies (Weng et al. 2019; Xu et al. 2023a, b). These studies show that at the same strain rate, the dynamic compressive strength and dynamic tensile strength of frozen sandstone increase as the frozen temperature decreases. However, compared with the frozen temperature, the strain rate may be a more critical factor in determining the dynamic strengths of frozen sandstone. In summary, previous studies have successfully revealed the effects of frozen temperature on the physical and mechanical characteristics of rock.

Apart from the physical and mechanical characteristics, the strengthening mechanism of the mechanical behavior of frozen rock has gradually attracted attention. It is widely accepted that the increase in mechanical strength of frozen rock is mainly due to the transformation of pore water into ice, which fills the original defects in rock and bears the external load together with rock matrix (Atkinson et al. 2018; Bai et al. 2020a, b). The freezing of pore water in rock is affected by various factors (Huang et al. 2018; Jia et al. 2019; Deprez et al. 2020), such as frozen temperature, pore size and pore pressure. The frozen temperature is an important factor responsible for the frozen degree of pore water in rock (Wang et al. 2021). Generally, the frozen degree of pore water increases as the frozen temperature decreases,

which is manifested as the variations in unfrozen water content and ice content (Weng et al. 2021, 2023). In previous studies, the variations in unfrozen water content and ice content of frozen rocks were investigated by various methods (Fabbri et al. 2006; Brunet et al. 2010; Murton et al. 2016; Kozlowski et al. 2016; Jia et al. 2019), such as time-domain reflectometry, dielectric capacity, differential scanning calorimetry, electrical resistivity tomography and nuclear magnetic resonance (NMR) technology. Among them, NMR technology has been widely used as an efficient, accurate and non-destructive method to study the distribution and content of unfrozen water in rock at low temperatures. For example, some studies performed a series of NMR tests to reveal the evolution of the unfrozen water content of sandstone during the freezing process (Weng et al. 2021, 2023). These studies show that as the temperature decreases from room temperature to − 25.0 °C, the unfrozen water content of sandstone first keeps approximately constant and then gradually decreases. The decrease in unfrozen water content indicates that more and more pore water is converted to ice. In particular, the decrease in unfrozen water content is significant in the range of 0.0 to − 5.0 °C. In addition, these studies also find that the speed of the solid–liquid phase transition of pore water and the total volume of ice are obviously affected by the pore size distribution of the sandstone. The water in pores with larger equivalent radius typically shows a faster freezing speed (Weng et al. 2021). Previous studies have successfully revealed the effects of temperature on the phase transition of pore water in rock and provided many good references and experience for investigating the strengthening mechanism of the mechanical characteristics of frozen rock. However, the relationship between the ice content and the mechanical characteristics of frozen rock has not been well established and further study is needed. In addition, the emerging in-situ NMR has the advantage of investigating the ice content of frozen rock at different temperatures. Therefore, it is necessary to study the effects of ice content on the mechanical properties of frozen sandstone by in-situ NMR technology.

This paper aims to study the effects of ice content in pores on the mechanical characteristics of frozen sandstone. The progressive freezing treatment and in-situ NMR test were performed to study the variation in ice content of a sandstone with temperature. Then, the freezing treatment, P-wave test and uniaxial compression test were performed to study the mechanical characteristics of frozen sandstone at different temperatures. Lastly, the effects of frozen degree of pore water on the mechanical characteristics of sandstone were discussed.

2 Material and methodology

2.1 Rock material

The rock material used in this study is a fresh red sandstone block retrieved from Hunan Province, China. Then, the mineral composition of the red sandstone and the proportion of various minerals were analyzed by performing the X-ray diffraction (XRD) test (Fig. 1). The red sandstone is composed of quartz (56.3%), k-feldspar (5.2%), plagioclase (16.5%), calcite (14.2%), clay mineral (7.4%) and other (0.4%).

2.2 Sample preparation

The cylindrical samples (Fig. 2) with a diameter of 25.0 mm and a height of 50.0 mm were cored from the red sandstone block in the same direction to avoid the anisotropy of rock material. Then, both ends of the cored samples were carefully polished to reduce the

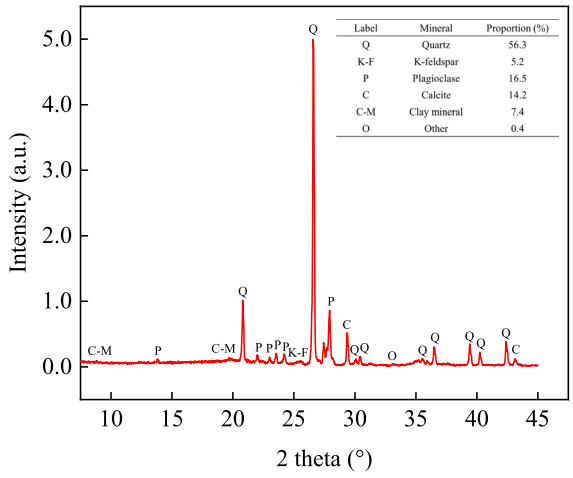

Fig. 1 Mineral composition and proportion of red sandstone

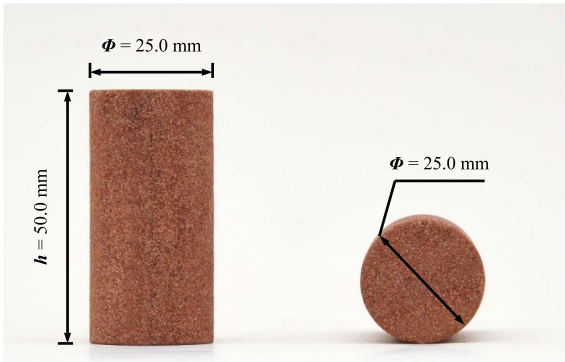

Fig. 2 Experimental sample

stress concentration during the loading. Subsequently, the polished samples were kept in a high-temperature furnace at 105.0 °C for 48 h and then naturally cooled to room temperature to obtain the dry samples. During the heating process, a constant heating rate (2.0 °C/min) was set to avoid thermal shock (Fan et al. 2021). After the dry treatment, the mechanical properties of the dry sample were tested. The density, P-wave velocity, UCS and elastic modulus of the dry sample are approximately 2.10 g/cm^3, 2719.67 m/s, 42.47 MPa and 9.09 GPa, respectively. Next, the dry samples with similar densities and P-wave velocities were selected to reduce the effects of sample differences on the experimental results and then placed in a vacuum-pressure saturation device for 48 h to obtain the water-saturated samples. Finally, the water-saturated samples were wrapped in cling film to prevent the moisture evaporation.

2.3 Experimental equipment

The experiments were conducted at the Rock Mechanics Laboratory of Beijing University of Technology. The main experimental equipment includes the SG-XL1200 high-temperature furnace, ZYB-II vacuum-pressure saturation device, GDW-100 low-temperature device, HS-YS2A rock wave velocity tester, SHT4605 electro-hydraulic servo universal testing machine and Niumag MesoMR14-060H-I LF-NMR system equipped with TES-NM65N-T temperature control device (Fig. 3). Noted that the NMR system equipped with the temperature control device can perform the in-situ NMR test on the sample at the target temperature, avoiding the effects of temperature changes on the test results.

2.4 Experimental procedure

Figure 3 also shows the experimental procedure of this study. After the dry and water-saturated treatments (step 1 of Fig. 3), two experimental works were conducted on the water-saturated sandstone sample (hereafter referred to as sandstone), namely the in-situ NMR test of sandstone under the progressive freezing treatment and the physical and mechanical properties tests of frozen sandstone with different temperatures. The detailed test methods are as follows.

To study the evolution of the ice content of sandstone with temperature, a series of in-situ NMR tests were performed on the sandstone under the progressive freezing treatment by the NMR system equipped with the temperature control device (step 2 of Fig. 3). The sandstone was gradually frozen from 25.0 to − 30.0 °C at a cooling rate of 2.0 °C/min. A total of nine temperature levels were set during the entire freezing process, namely 25.0 °C, 0.0 °C, − 2.5 °C, − 5.0 °C, − 10.0 °C, − 15.0 °C, − 20.0 °C, − 25.0 °C and − 30.0 °C. When the temperature reached the preset level, the sandstone was held at the current temperature for 4 h to ensure thermal equilibrium. Figure 4 shows the freezing process of pore water in sandstone within 4 h at − 5.0 °C. As the frozen time increases to 4 h, the transverse relaxation time (T_2) distribution curve of the pore water in sandstone first shifts downward and left and then remains stable (Fig. 4a). Correspondingly, as the frozen time increases, the T_2 peak area first rapidly decreases and then remains almost constant (Fig. 4b). The variations in the T_2 distribution curve and T_2 peak area with frozen time prove that the sandstone can achieve thermal equilibrium within 4 h. When the frozen time reached 4 h, the in-situ NMR test was conducted on the sandstone to obtain the T_2 distribution of pore water in sandstone at the current temperature. Subsequently, the temperature was decreased to the next preset level and then the above processes were repeated to obtain the T_2 distribution of pore water in sandstone at different temperatures. During the in-situ NMR test, the temperature of the magnet was kept at 32.0 ± 0.02 °C, the temperature of the probe coil was kept at 25.0 ± 0.50 °C, the test sequence was Carr-Purcell-Meiboom-Gill (CPMG) (Carr and Purcell. 1954; Meiboom and Gill. 1958; Liu et al. 2020), the resonance frequency was 12 MHz, the echo interval

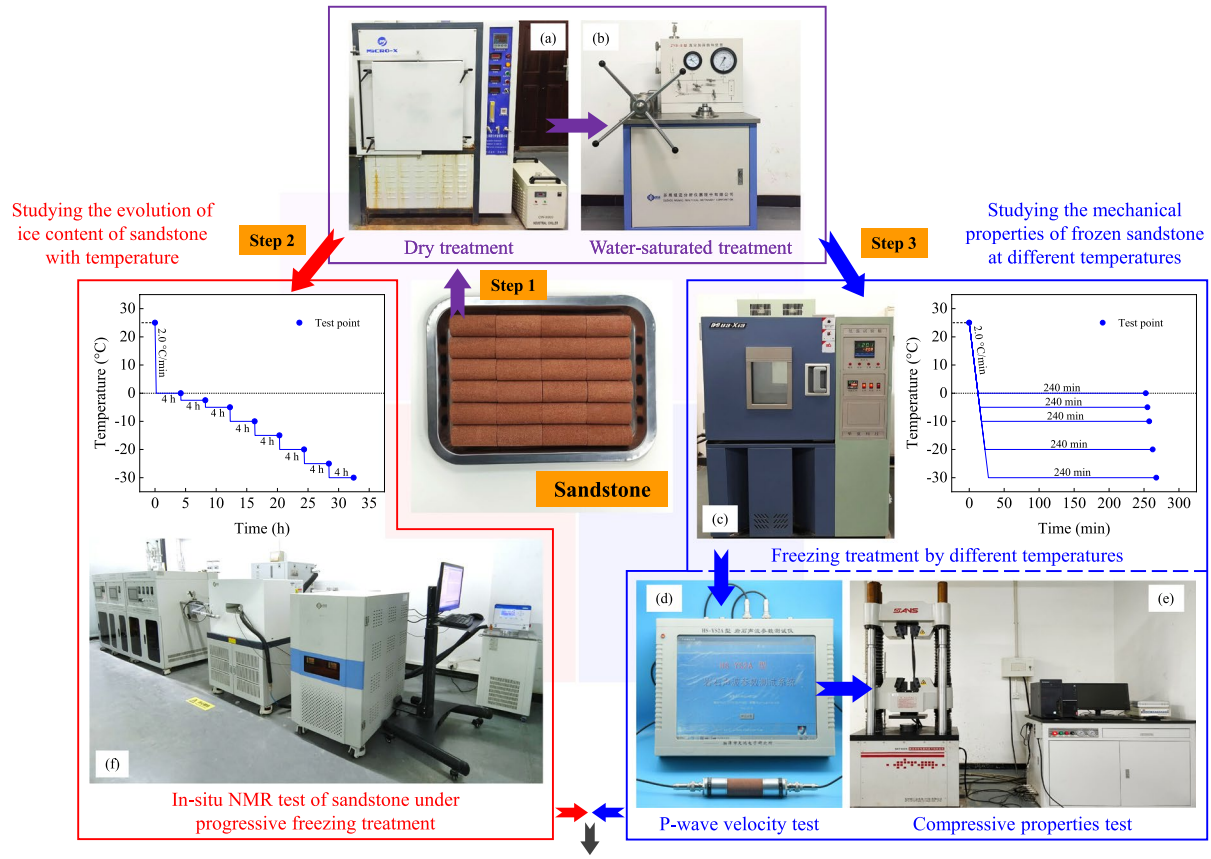

Fig. 3 Schematic of experimental procedure and equipment. **a** SG-XL1200 high-temperature furnace; **b** ZYB-II vacuum-pressure saturation device; **c** GDW-100 low-temperature device; **d** HS-YS2A rock wave velocity tester; **e** SHT4605 electro-hydraulic servo universal testing machine; **f** Niumag MesoMR14-060H-I LF-NMR system equipped with TES-NM65N-T temperature control device

was set to 0.20 ms, the number of echoes was 3200 and the accumulated sampling times were 64. Noted that the T_2 of hydrion in solid materials, such as rock and ice, is extremely short (typically less than 5 μm) and much smaller than that of hydrion in water (Zhao et al. 2017; Weng et al. 2021). The signals from ice are barely detectable at low magnetic fields (Wang et al. 2021). Therefore, it is considered that the intensity of NMR signals of frozen sandstone comes from the unfrozen pore water. Therefore, the unfrozen water and ice in frozen sandstone can be further distinguished based on this principle. In addition, a total of three samples were prepared for this work to avoid experimental dispersion.

To study the physical and mechanical characteristics of frozen sandstone at different temperatures, the freezing treatment, P-wave velocity test and uniaxial compression experiment were conducted on the sandstone successively (step 3 of Fig. 3). First, the freezing treatment was performed on the sandstone to obtain the frozen sandstone. In this process, the target temperatures were set to 25.0 °C, 0.0 °C, − 5.0 °C, − 10.0 °C, − 20.0 °C and − 30.0 °C, respectively. Similarly, the cooling rate was 2.0 °C/min and the frozen time was 4 h to ensure the thermal equilibrium. Right after the sandstone was maintained at the preset temperature for 4 h, the P-wave velocity test and uniaxial compression experiment were performed on the frozen sandstone.

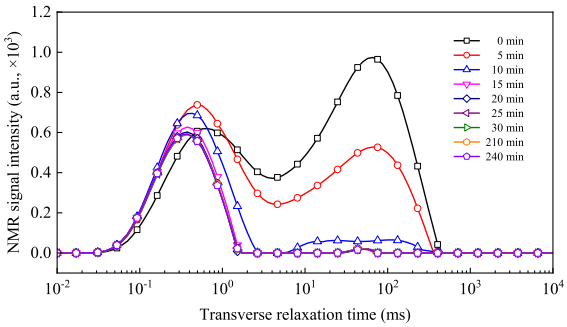

(a) Variation in T_2 distribution curve of sample with frozen time

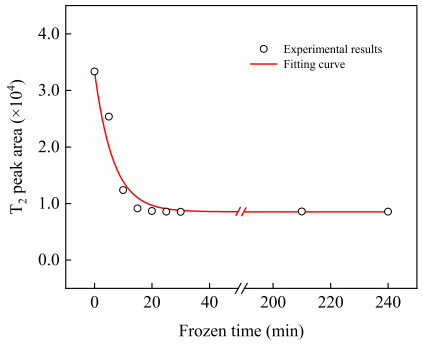

(b) Variation in T_2 peak area of sample with frozen time

Fig. 4 Example of phase transition process of water in sandstone (−5.0 °C, 4 h)

In the uniaxial compression test, the loading mode was stress control with a loading rate of 0.25 MPa/s. In addition, three samples were prepared for each target temperature to avoid experimental dispersion.

3 Results and discussion

3.1 Evolution of ice content of sandstone with temperature

3.1.1 T_2 distribution of water in sandstone at different temperatures

Considering the similarity of the T_2 distribution patterns of the three samples, sample 1 is taken as an example to analyze the variation of water distribution of sandstone as the temperature decreases. In previous studies, pore water in porous rocks was usually classified into bound water, capillary water and bulk water based on the corresponding T_2 values (Coates et al. 1998; Godefroy et al. 2001). For the sandstone, the T_2 value of bound water is less than 3 ms, the T_2 value of capillary water is in the range of 3 ms to 33 mm and the T_2 value of bulk water is larger than 33 ms (Jia et al. 2019; Weng et al. 2021). Therefore, the two critical T_2 values (3 ms and 33 ms) are adopted in this study to divided the pore water of sandstone. Figure 5 shows the variation of T_2 distribution curve of sandstone with temperature and Table 1 shows the corresponding T_2 peak area obtained by integrating the T_2 distribution curve. As the temperature decreases from 25.0 to − 30.0 °C, the T_2 distribution curve shifts downward and left and changes from a bimodal mode to a unimodal mode. Accordingly, the T_2 peak area first decreases significantly and then decreases slowly. As the temperature decreases from 25.0 to 0.0 °C, the T_2 distribution curve changes slightly and exhibits a bimodal mode, indicating that the vast majority of the pore water in sandstone remains unfrozen. Then, as the temperature decreases from 0.0 to − 2.5 °C, the T_2 distribution curve changes from bimodal mode to unimodal mode with the left peak shifting to the left and the right peak decreasing to nearly zero. Accordingly, the T_2 peak area decreases by 71.07% from 34,226.55 to 9902.55. This phenomenon indicates that most of the pore water in sandstone, especially the bulk and capillary water, is converted to ice when the temperature decreases to − 2.5 °C. Interestingly, some bound water is still in an unfrozen state at − 2.5 °C. As the temperature continues to decrease, the left peak of the T_2 distribution curve gradually shifts downward and the corresponding T_2 peak area slowly decreases. This indicates that the bound water in sandstone gradually transforms into ice. However, even when the

Table 1 T_2 peak area of three samples at different temperatures

Temperature (°C)	T_2 peak area		
	Sample 1	Sample 2	Sample 3
25.0	34,640.95	34,850.71	35,988.73
0.0	34,226.55	34,360.12	35,654.25
− 2.5	9902.55	10,235.10	10,740.01
− 5.0	8717.97	8990.77	9169.28
− 10.0	6474.87	6787.38	6956.26
− 15.0	4978.30	5251.31	5270.34
− 20.0	3864.82	4135.96	4152.15
− 25.0	3024.59	3411.31	3347.75
− 30.0	2321.75	2731.75	2717.73

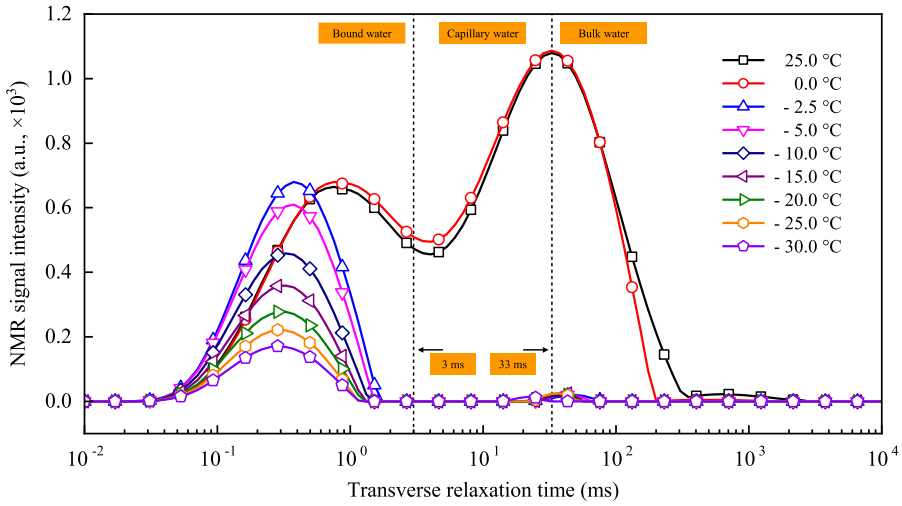

Fig. 5 Variation in T_2 distribution of water in sandstone as temperature

temperature decreases to − 30 °C, there is still some unfrozen bound water in the sandstone. This phenomenon has also been found in previous research (Jia et al. 2019; Su et al. 2022). These studies also find that some water in rocks doesn't freeze within a certain negative temperature range. In fact, the freezing of pore water is determined by various factors (Huang et al. 2018; Jia et al. 2019; Deprez et al. 2020), such as frozen temperature, pore size and pore pressure. Especially, the water in small pores of rock requires a lower temperature to freeze (Weng et al. 2021).

3.1.2 *Variation in frozen ratio of sandstone with temperature*

The frozen ratio was introduced to quantitatively characterize the frozen degree of pore water in sandstone under low-temperature environments, which was defined as the percentage of the mass of ice in sandstone to the total mass of water in sandstone. The total mass of water in sandstone was measured after water-saturated treatment. The mass of ice was the difference between the total mass of water and the mass of unfrozen water. Therefore, the frozen ratio of sandstone can also be expressed as

$$R_f = \frac{m_{tot} - m_{unf}}{m_{tot}} \times 100\% \quad (1)$$

where R_f is the frozen ratio of sandstone, m_{tot} is the total mass of water in sandstone, m_{unf} is the mass of unfrozen water in sandstone.

The mass of unfrozen water and ice in sandstone is difficult to measure by directly using traditional methods. However, the unfrozen water in sandstone at low temperatures can be reflected by the T_2 distribution curve (Godefroy et al. 2001; Weng et al. 2021), as shown in Sect. 3.1.1. Moreover, these studies found that the relationship between T_2 peak area and water mass in sandstone can be expressed by a linear function. In this study, the water-soaking treatment and NMR test were conducted on the sandstone to obtain the linear relationship as

$$S_{wat} = a_0 \cdot m_{wat} \quad (2)$$

where S_{wat} is the T_2 peak area of water in sandstone, m_{wat} is the mass of water in sandstone and a_0 is the calculation parameter ($a_0 = 9981.52$ and $R^2 = 0.99$).

Figure 6 shows the relationship between T_2 peak area and mass of water in sandstone. It can be seen that the linear function can describe this relationship well with R^2 as high as 0.99. Therefore, the frozen ratio of sandstone can be further expressed as

$$R_f = \frac{S_{tot} - S_{unf}}{S_{tot}} \times 100\% \quad (3)$$

where S_{tot} is the T_2 peak area of all water in sandstone, S_{unf} is the T_2 peak area of unfrozen water in sandstone.

According to the above method, the frozen ratio of sandstone at different temperatures can be

obtained. Figure 7 shows the variation of frozen ratio of sandstone with temperature. Noted that the frozen ratio in this figure is the average of the three samples. As the temperature decreases from 25.0 to − 30.0 °C, the frozen ratio first remains approximately constant, then increases sharply and finally increases slowly. For the positive temperature stage, the water in sandstone is always in an unfrozen state, resulting in a constant frozen ratio of 0.00%. When the temperature reaches 0.0 °C, the frozen ratio remains approximately constant (it actually only increases to 1.18%), indicating that the vast majority of the pore water in sandstone is still in an unfrozen state at this temperature. Then, for the negative temperature stage, the frozen ratio shows a monotonically increasing trend as the temperature decreases. As the temperature decreases from 0.0 to − 2.5 °C, the frozen ratio increases sharply from 1.18 to 70.73%, an increase of 5894.07%. This phenomenon indicates that most of the pore water in sandstone is transformed into ice in the range of 0.0 to − 2.5 °C. Interestingly, it can be seen that for the sandstone materials, there may be a critical frozen temperature within the range of 0.0 to − 2.5 °C, which leads to the sudden phase transition of pore water. Actually, previous studies have found that the critical frozen temperature of water-saturated sandstone is about − 0.97 °C (Jia et al. 2019; Weng et al. 2021). Subsequently, as the temperature decreases from − 2.5 to − 10.0 °C, the frozen ratio increases by 14.28% from 70.73 to 80.83%. As the temperature decreases from − 10.0 to − 20.0 °C, the frozen ratio increases by 9.46% from 80.83 to 88.48%. As the temperature decreases from − 20.0 to − 30.0 °C, the frozen ratio increases by 4.70% from 88.48 to 92.64%. The frozen ratio continuously increases as the temperature decreases, but the rate of increase gradually slows down.

According to the above analysis, the pore water in sandstone mainly experiences three stages as the temperature decreases from 25.0 to − 30.0 °C, which are stable liquid (from 25.0 to 0.0 °C), sharp solid–liquid phase change (from 0.0 to − 2.5 °C) and slow solid–liquid phase change (from − 2.5 to − 30.0 °C). Therefore, to describe the changing process, the relationship between the frozen ratio and the temperature was established by a piecewise function as

$$R_f(T) = \begin{cases} 0 & T > 0 \\ \frac{A+BT}{1+CT+DT^2} & T \le 0 \end{cases} \quad (4)$$

where $R_f(T)$ is the frozen ratio of sandstone at T °C, T is the temperature, A, B, C and D are the calculation parameters.

The fitting results and calculation parameters are presented in Fig. 7 and Table 2. It can be seen that the fitting results are satisfying with R^2 as high as 0.99, indicating that the piecewise function can well describe the relationship between frozen ratio and

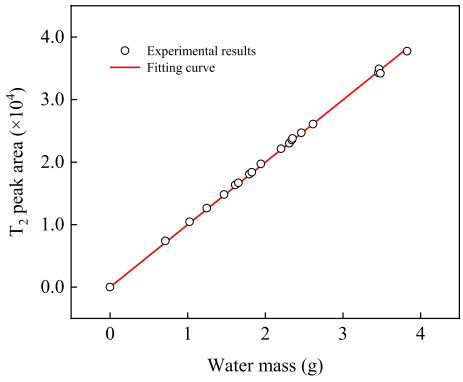

Fig. 6 Relationship between T_2 peak area and mass of water in sandstone

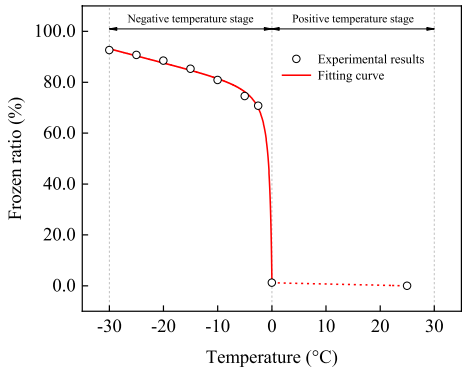

Fig. 7 Variation in the frozen ratio of sandstone as temperature

Table 2 Calculation parameters of frozen ratio model of sandstone

A	B	C	D	R^2
1.19	− 185.24	− 2.29	− 0.01	0.99

Table 3 Estimated results of frozen ratio at different temperatures

Temperature (°C)	25.0	0.0	− 5.0	− 10.0	− 20.0	− 30.0
Frozen ratio (%)	0.00	1.19	76.25	81.41	87.57	93.18

temperature. This function was used to estimate the frozen ratio of sandstone at specific temperatures (25.0 °C, 0.0 °C, − 5.0 °C, − 10.0 °C, − 20.0 °C and − 30.0 °C) in the subsequent experiments. The estimated results of the frozen ratio at different temperatures are presented in Table 3.

3.2 Effects of frozen ratio on mechanical properties of sandstone

3.2.1 P-wave velocity of sandstone

Figure 8a shows the variation in the P-wave velocity of sandstone with the temperature decreases. The P-wave velocity first remains approximately constant as the temperature decreases from 25.0 to 0.0 °C. Then, the P-wave velocity increases sharply as the temperature decreases from 0.0 to − 5.0 °C. Finally, as the temperature decreases from − 5.0 to − 30.0 °C, the P-wave velocity continuously increases, but the rate of increase slows down. It is interesting that as the temperature decreases, the changing trend of the P-wave velocity is similar to that of the frozen ratio, indicating that the P-wave velocity may be a potential parameter for evaluating the frozen degree of pore water in sandstone at low temperatures. Figure 8b shows the effects of the frozen ratio on the P-wave velocity of sandstone. The P-wave velocity shows a monotonically increasing trend as the frozen ratio increases. As the frozen ratio increases from 0.00 to 76.25%, the P-wave velocity of sandstone increases by 27.49% from 3366.67 to 4292.33 m/s. In this stage, most of the pore water in sandstone is converted into ice, which causes the obvious increase in P-wave velocity, because the ultrasonic velocity in solid (ice) is much faster than that in liquid (water). Then, as the frozen ratio increases from 76.25 to 81.41%, the P-wave velocity increases by 4.78% from 4292.33 to 4497.33 m/s. Subsequently, as the frozen ratio increases from 81.41 to 87.57%, the P-wave velocity increases by 3.74% from 4497.33 m/s to 4665.67% m/s. Finally, as the frozen ratio increases from 87.57 to 93.18%, the P-wave velocity increases by 2.05%

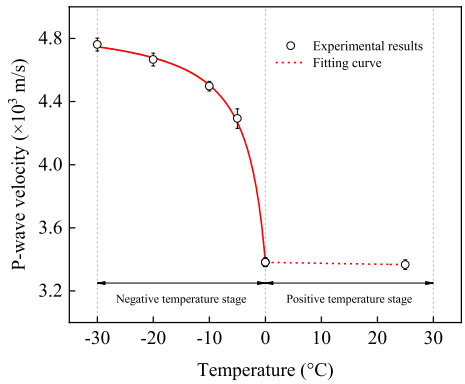

(a) Variation in P-wave velocity of sandstone as temperature

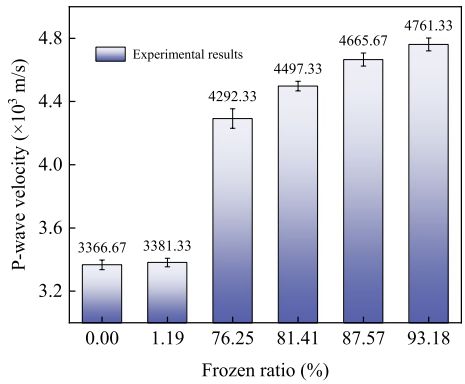

(b) P-wave velocities of sandstone with different frozen ratios

Fig. 8 Effects of frozen ratio on P-wave velocity of sandstone

from 4665.67 to 4761.33 m/s. Therefore, the frozen degree of pore water in sandstone obviously affects the P-wave velocity. The infill effect of ice may play an important role in the increasing of P-wave velocity (Inada and Yokota. 1984; Draebing and Krautblatter. 2012).

3.2.2 Compressive characteristics of sandstone

Figure 9 shows the stress–strain curves of sandstone with different frozen ratios. The stress–strain curve of sandstone gradually shifts upward and rightward as the increase of frozen ratio, indicating that the frozen degree of pore water in sandstone affects the

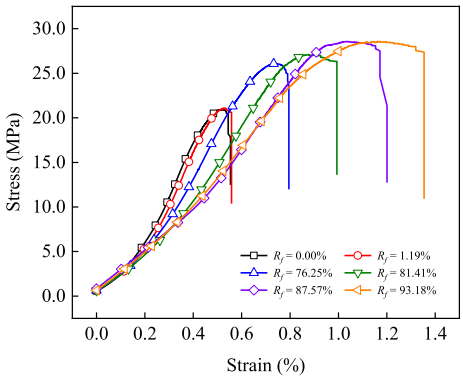

Fig. 9 Stress–strain curves of sandstone with different frozen ratios

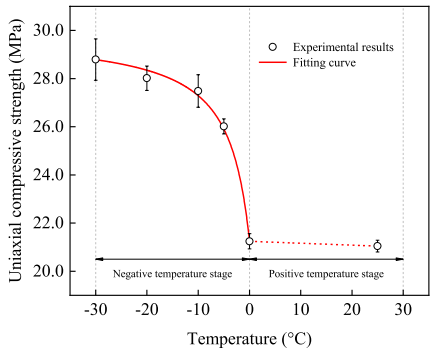

(a) Variation in uniaxial compressive strength of sandstone as temperature

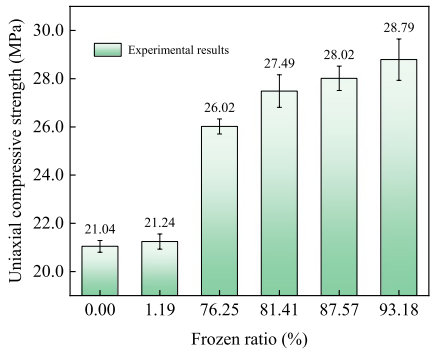

(b) Uniaxial compressive strengths of sandstone with different frozen ratios

Fig. 10 Effects of frozen ratio on uniaxial compressive strength of sandstone

mechanical behavior of sandstone under uniaxial compression. Obviously, the peak stress of sandstone increases with the frozen ratio increases, indicating that the freezing of pore water in sandstone improves the bearing capacity of sandstone under uniaxial compression. Moreover, the peak strain (the strain corresponding to the peak stress) gradually increases as the frozen ratio increases, indicating that the axial deformation of sandstone increases with the frozen degree of pore water. Interestingly, the failure mode of sandstone gradually transforms from brittle to ductile as the frozen ratio increases.

Figure 10a shows the variation in the UCS of sandstone with temperature. The UCS of sandstone remains approximately constant as the temperature decreases from 25.0 to 0.0 °C. Then, the UCS gradually increases as the temperature decreases from 0.0 to − 30.0 °C, indicating that the sandstone has a stronger bearing capacity in low-temperature environments. Especially, as the temperature decreases from 0.0 to − 2.5 °C, the UCS increases from 21.24 to 26.02 MPa and the enhancement effects of low temperature are most significant. Figure 10b shows the effects of the frozen ratio on the UCS of sandstone. The UCS of sandstone increases monotonically as the frozen ratio increases. As the frozen ratio increases from 0.00 to 76.25%, the UCS increases by 23.67% from 21.04 to 26.02 MPa. Then, as the frozen ratio increases from 76.25 to 81.41%, the UCS increases by 5.65% from 26.02 to 27.49 MPa. Subsequently, as the frozen ratio increases from 81.41 to 87.57%, the UCS increases by 1.93% from 27.49 MPa to 28.02% MPa. Finally, as the frozen ratio increases from 87.57 to 93.18%, the UCS increases by 2.75% from 28.02 to 28.79 MPa. Therefore, the frozen degree of pore water has significant effects on the bearing capacity of sandstone under uniaxial compression. The increase in frozen ratio means that more and more water in sandstone transforms into ice, which shares the external loads with the sandstone matrix (Yamabe and Neaupane. 2001; Bai et al. 2020a, b). This phenomenon may be the main reason for the increase in UCS.

Figure 11a shows the variation in the peak strain of sandstone as the decrease of temperature. Noted that the peak strain is the strain corresponding to the UCS of sandstone. As the decrease of temperature, the peak strain of sandstone first keeps constant and then increases obviously. Figure 11b presents the effects of the frozen ratio on the peak strain of sandstone. As the frozen ratio increases from 0.00 to 76.25%, the peak strain increases by 42.31% from 0.52 to 0.74%. Next, as the frozen ratio increases from 76.25 to 81.41%, the peak strain increases by 18.92% from 0.74 to 0.88%. Subsequently, as the frozen ratio

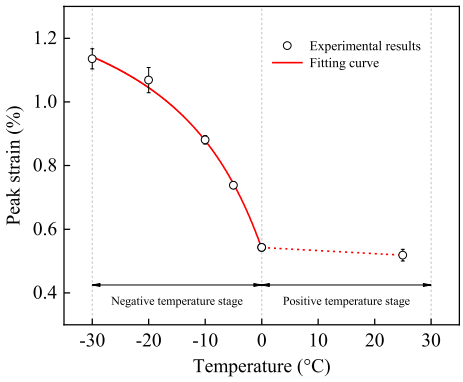

(a) Variation in peak strain of sandstone as temperature

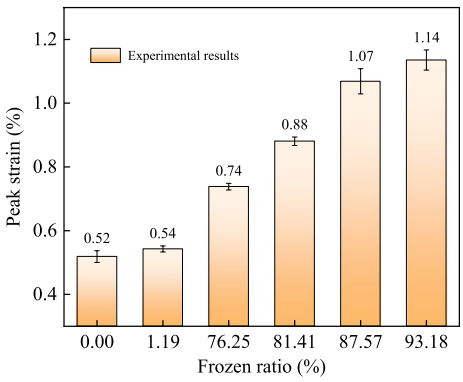

(b) Peak strains of sandstone with different frozen ratios

Fig. 11 Effects of frozen ratio on peak strain of sandstone

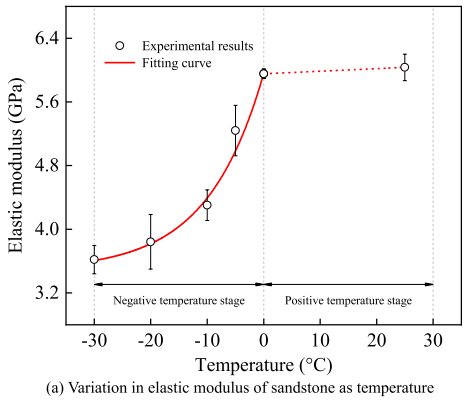

(a) Variation in elastic modulus of sandstone as temperature

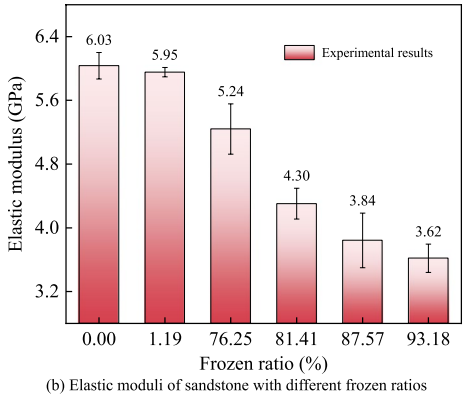

(b) Elastic moduli of sandstone with different frozen ratios

Fig. 12 Effects of frozen ratio on elastic modulus of sandstone

increases from 81.41 to 87.57%, the peak strain increases by 21.59% from 0.88 to 1.07%. Finally, as the frozen ratio increases from 87.57 to 93.18%, the peak strain increases by 6.54% from 1.07 to 1.14%. The increase in peak strain means that the axial deformation of sandstone under uniaxial compression gradually increases as the frozen degree of pore water increases.

Figure 12a shows the variation in the elastic modulus of sandstone as the temperature decreases. It is found that as the temperature decreases from 25.0 to 0.0 °C, the elastic modulus of sandstone remains constant. Then, the elastic modulus gradually decreases as the temperature decreases from 0.0 to − 30.0 °C. Figure 12b presents the effects of the frozen ratio on the elastic modulus of sandstone. As the frozen ratio increases from 0.00 to 76.25%, the elastic modulus decreases by 13.10% from 6.03 to 5.24 GPa. Then, as the frozen ratio increases from 76.25 to 81.41%, the elastic modulus decreases by 17.94% from 5.24 to 4.30 GPa. Subsequently, as the frozen ratio increases from 81.41 to 87.57%, the elastic modulus decreases by 10.70% from 4.30 to 3.84 GPa. Finally, as the frozen ratio increases from 87.57 to 93.18%, the elastic modulus decreases by 5.73% from 3.84 to 3.62 GPa.

4 Conclusions

This paper investigated the ice content of sandstone at different temperatures and analyzed the effects of ice content on the mechanical characteristics of sandstone. First, the progressive freezing treatment and in-situ NMR test were conducted. Then, the mechanical properties of sandstone with different temperatures were tested. Finally, the effects of the frozen degree of pore water on the mechanical properties of sandstone were discussed. The conclusions obtained are as follows.

(1) The pore water in sandstone mainly shows three stages as the temperature decreases from 25.0 to − 30.0 °C, which are stable liquid (from 25.0 to

0.0 °C), sharp solid–liquid phase transition (from 0.0 to − 2.5 °C) and slow solid–liquid phase transition (from − 2.5 to − 30.0 °C), respectively. Correspondingly, as the temperature decreases, the frozen ratio of sandstone first remains approximately constant, then increases rapidly and finally increases slowly. Particularly, the bulk and capillary water in sandstone is rapidly frozen in the range of 0.0 to − 2.5 °C, leading to a significant increase in the frozen ratio. Moreover, even if the temperature decreases to − 30 °C, there is still bound water in sandstone that cannot be frozen.

(2) The low temperature significantly affects the mechanical behavior of sandstone. As the temperature decreases, the P-wave velocity, UCS and peak strain increase while the elastic modulus decreases.

(3) As the frozen ratio of sandstone increases from 0.00% to 93.18%, the P-wave velocity, UCS and peak strain increase by 41.43%, 36.83% and 119.23% while the elastic modulus decreases by 39.97%, indicating that the frozen degree of pore water has obvious effects on the compressive properties of sandstone.

(4) It is interesting that as the increase of frozen ratio, the failure mode of the sandstone under uniaxial compression gradually transforms from brittle to ductile.

Author contribution Each author has contributed to this study. LFF provided the research idea and plan. XLD improved the research idea and plan. BQ conducted the experiments and wrote the manuscript. CMM and QHY assisted in the experiments and data analysis. All authors have reviewed the manuscript.

Funding This work is supported by the National Natural Science Foundation of China (No. 12172019) and Beijing Natural Science Foundation (JQ20039).

Data availability The data are contained within this manuscript.

Declarations

Competing interests The authors declare no competing interests.

Ethics approval Not applicable.

Consent for publcation All authors agree to publish this manuscript.

References

Abdulagatova ZZ, Abdulagatov IM, Emirov SN (2010) Effect of pressure, temperature, and oil-saturation on the thermal conductivity of sandstone up to 250MPa and 520K. J Petrol Sci Eng 73(1):141–155

Abdulagatova ZZ, Kallaev SN, Omarov ZM, Bakmaev AG, Grigor Ev BA, Abdulagatov IM (2020) Temperature effect on thermal-diffusivity and heat-capacity and derived values of thermal-conductivity of reservoir rock materials. Geomech Geophys Geo 6(1):8

Atkinson J, Durham WB, Seager S (2018) The strength of ice-saturated extraterrestrial rock analogs. Icarus 315:61–68

Bai Y, Shan RL, Ju Y, Wu YX, Sun PF, Wang ZE (2020a) Study on the mechanical properties and damage constitutive model of frozen weakly cemented red sandstone. Cold Reg Sci Technol 171:102980

Bai Y, Shan RL, Ju Y, Wu YX, Tong X, Han TY, Dou HY (2020b) Experimental study on the strength, deformation and crack evolution behaviour of red sandstone samples containing two ice-filled fissures under triaxial compression. Cold Reg Sci Technol 174:103061

Brunet P, Clement R, Bouvier C (2010) Monitoring soil water content and deficit using Electrical Resistivity Tomography (ERT)—a case study in the Cevennes area. France J Hydrol 380(1):146–153

Carr HY, Purcell EM (1954) Effects of diffusion on free precession in nuclear magnetic resonance experiments. Phys Rev 94(3):630–638

Chen GQ, Guo TY, Serati M, Pei BC (2022) Microcracking mechanisms of cyclic freeze-thaw treated red sandstone: Insights from acoustic emission and thin-section analysis. Constr Build Mater 329:127097

Chen B, Shen BT, Jiang HY (2023) Shear behavior of intact granite under thermo-mechanical coupling and three-dimensional morphology of shear-formed fractures. J Rock Mech Geotech 15(3):523–537

Coates GR, Galford J, Mardon D, Marschall D (1998) A new characterization of bulk-volume irreducible using magnetic resonance. Log Anal 39(1):51–63

Deprez M, De Kock T, De Schutter G, Cnudde V (2020) A review on freeze-thaw action and weathering of rocks. Earth-Sci Rev 203:103143

Draebing D, Krautblatter M (2012) P-wave velocity changes in freezing hard low-porosity rocks: a laboratory-based time-average model. Cryosphere 6(5):1163–1174

Fabbri A, Fen-Chong T, Coussy O (2006) Dielectric capacity, liquid water content, and pore structure of thawing-freezing materials. Cold Reg Sci Technol 44(1):52–66

Fan LF, Wu ZJ, Wan Z, Gao JW (2017) Experimental investigation of thermal effects on dynamic behavior of granite. Appl Therm Eng 125:94–103

Fan LF, Gao JW, Wu ZJ, Yang SQ, Ma GW (2018) An investigation of thermal effects on micro-properties of granite by X-ray CT technique. Appl Therm Eng 140:505–519

Fan LF, Gao JW, Du XL, Wu ZJ (2020) Spatial gradient distributions of thermal shock-induced damage to granite. J Rock Mech Geotech 12(5):917–926

Fan LF, Yang KC, Wang M, Wang LJ, Wu ZJ (2021) Experimental study on wave propagation through granite after high-temperature treatment. Int J Rock Mech Min 148:104946

Godefroy S, Korb JP, Fleury M, Bryant RG (2001) Surface nuclear magnetic relaxation and dynamics of water and oil in macroporous media. Phys Rev E 64(2 Pt 1):21605

Huang SB, Liu QS, Liu YZ, Ye ZY, Cheng AP (2018) Freezing strain model for estimating the unfrozen water content of saturated rock under low temperature. Int J Geomech 18(2):04017137

Huang SB, Liu F, Liu G, Yu SL (2023) Estimation of the unfrozen water content of saturated sandstones by ultrasonic velocity. Int J Min Sci Techno. https://doi.org/10.1016/j.ijmst.2023.02.003

Inada Y, Yokota K (1984) Some studies of low temperature rock strength. Int J Rock Mech Min 21(3):145–153

Jia HL, Ding S, Wang Y, Zi F, Sun Q, Yang GS (2019) An NMR-based investigation of pore water freezing process in sandstone. Cold Reg Sci Technol 168:102893

Kodama J, Goto T, Fujii Y, Hagan P (2013) The effects of water content, temperature and loading rate on strength and failure process of frozen rocks. Int J Rock Mech Min 62:1–13

Kozlowski T (2016) A simple method of obtaining the soil freezing point depression, the unfrozen water content and the pore size distribution curves from the DSC peak maximum temperature. Cold Reg Sci Technol 122:18–25

Li B, Huang LS, Lv XQ, Ren YJ (2021) Variation features of unfrozen water content of water-saturated coal under low freezing temperature. Sci Rep-Uk 11(1):15398

Liu ZS, Liu DM, Cai YD, Yao YB, Pan ZJ, Zhou YF (2020) Application of nuclear magnetic resonance (NMR) in coalbed methane and shale reservoirs: a review. Int J Coal Geol 218:103261

Lu CF, Cai CX (2019) Challenges and countermeasures for construction safety during the Sichuan-Tibet railway project. Engineering 5(5):833–838

Maji V, Murton JB (2021) Experimental observations and statistical modeling of crack propagation dynamics in limestone by acoustic emission analysis during freezing and thawing. J Geophys Res-Earth 126(7):e2021JF006127

Matsuoka N (1990) Mechanisms of rock breakdown by frost action: an experimental approach. Cold Reg Sci Technol 17(3):253–270

Meiboom S, Gill D (1958) Modified spin-echo method for measuring nuclear relaxation times. Rev Sci Instrum 29(8):688–691

Murton JB, Kuras O, Krautblatter M, Cane T, Tschofen D, Uhlemann S, Schober S, Watson P (2016) Monitoring rock freezing and thawing by novel geoelectrical and acoustic techniques. J Geophys Res-Earth 121(12):2309–2332

Ozbek A (2014) Investigation of the effects of wetting-drying and freezing-thawing cycles on some physical and mechanical properties of selected ignimbrites. B Eng Geol Environ 73(2):595–609

Park C, Synn JH, Shin HS, Cheon DS, Lim HD, Jeon SW (2004) An experimental study on the thermal characteristics of rock at low temperatures. Int J Rock Mech Min 41(3):367–368

Shan RL, Song YW, Song LW, Bao Y (2019) Dynamic property tests of frozen red sandstone using a split hopkinson pressure bar. Earthq Eng Eng Vib 18(3):511–519

Shen YJ, Wang YZ, Zhao XD, Yang GS, Jia HL, Rong TL (2018) The influence of temperature and moisture content on sandstone thermal conductivity from a case using the artificial ground freezing (AGF) method. Cold Reg Sci Technol 155:149–160

Su ZZ, Tan XJ, Chen WZ, Jia HL, Xu F (2022) A model of unfrozen water content in rock during freezing and thawing with experimental validation by nuclear magnetic resonance. J Rock Mech Geotech 14(5):1545–1555

Wang T, Sun Q, Jia HL, Ren JT, Luo T (2021) Linking the mechanical properties of frozen sandstone to phase composition of pore water measured by LF-NMR at subzero temperatures. B Eng Geol Environ 80(6):4501–4513

Weng L, Wu ZJ, Liu QS, Wang ZY (2019) Energy dissipation and dynamic fragmentation of dry and water-saturated siltstones under sub-zero temperatures. Eng Fract Mech 220:106659

Weng L, Wu ZJ, Liu QS, Chu ZF, Zhang SL (2021) Evolutions of the unfrozen water content of saturated sandstones during freezing process and the freeze-induced damage characteristics. Int J Rock Mech Min 142:104757

Weng L, Wu ZJ, Chu ZF, Lu HF, Xu XY, Liu QS (2023) Evolution of the unfrozen water content for partially-saturated sandstones and the critical degree of saturation. Rock Mech Rock Eng 56(1):1–18

Wu QB, Zhang TJ, Liu YZ (2010) Permafrost temperatures and thickness on the Qinghai-Tibet Plateau. Global Planet Change 72(1):32–38

Wu J, Lu YN, Wang KB, Cai Y, Xiao C (2023) Combined effects of freeze-thaw cycles and chemical corrosion on triaxial mechanical properties of sandstone. Geomech Geophys Geo 9(1):57

Xu JC, Pu H, Sha ZH (2022) Dynamic mechanical behavior of the frozen red sandstone under coupling of saturation and impact loading. Appl Sci-Basel 12(15):7767

Xu Y, Fu Y, Yang YX, Yao W, Xia KW, Peng JB (2023a) Dynamic compression properties of a saturated white sandstone under ambient sub-zero temperatures. Acta Geotech. https://doi.org/10.1007/s11440-023-01836-1

Xu Y, Yang Y, Li X, Wu B, Yao W (2023b) Dynamic compressive test of saturated sandstones under ambient sub-zero temperature. Exp Mech 63(1):191–200

Yamabe T, Neaupane KM (2001) Determination of some thermo-mechanical properties of Sirahama sandstone under subzero temperature condition. Int J Rock Mech Min 38(7):1029–1034

Zhang YL, Zhao GF (2020) A global review of deep geothermal energy exploration: from a view of rock mechanics and engineering. Geomech Geophys Geo 6(1):1–26

Zhao YX, Sun YF, Liu SM, Wang K, Jiang YD (2017) Pore structure characterization of coal by NMR cryoporometry. Fuel 190:359–369

Zhao ZH, Sun W, Chen SJ, Yin DW, Liu H, Chen BS (2021) Determination of critical criterion of tensile-shear failure in Brazilian disc based on theoretical analysis and meso-macro numerical simulation. Comput Geotech 134:104096

Zhong WL, Zhang YH, Fan LF (2023) High-ductile engineered geopolymer composites (EGC) prepared by calcined natural clay. J Build Eng 63:105456